SILVER NANOPARTICLE LOADED ON ACTIVATED CARBON AS AN ADSORBENT FOR THE REMOVAL OF SUDAN RED 7B FROM AQUEOUS SOLUTION

Farzaneh Marahel[1,*], Mehrorang Ghaedi[1] and Syamak Nasiri Kokhdan[2]

[1] Chemistry Department, Islamic Azad University, Omidiyeh Branch, Omidiyeh, Iran
[2] Young Researchers club, Yasooj Branch, Islamic Azad University, Yasooj, Iran

ABSTRACT

In this research adsorption and removal of Sudan red 7B (SR7B) from aqueous solution using silver nanoparticle loaded on activated carbon (Ag-NP-AC) has been investigated. Equilibrium data are mathematically modeled using the Freundlich Langmuir, Tempkin and Dubinin-Radushkevich (D–R) adsorption models. The SR7B adsorption kinetics on to Ag-NP-AC was studied in terms of pseudo-first-order, pseudo-second-order, Intraparticle diffusion and Elovich models. A maximum adsorption capacity of 90.909 $mg.g^{-1}$ based on Langmuir as most applicable model at equilibrium is achieved. The high capacity and low removal time show the suitability and usefulness of Ag-NP-AC alternative adsorbent for the removal of SR7B in wastewater treatment.

KEYWORDS: Sudan red 7B (SR7B); Silver nanoparticle loaded on activated carbon (Ag-NP- AC); Kinetic.

1. INTRODUCTION

Dyes as multiple varieties generally resist the breakdown of long-term exposure to sunlight, water and other atrocious conditions. Therefore, the dye treatment of wastewater is a difficult task. Azo dyes among overall category of synthetic textile dyestuffs consist of half of global production and during dyeing operation processes emerged to wastewaters [1]. The removal of dye (as widely applicable modern industry) from textile effluents is one of the most significant environmental problems synthetic origin and complex aromatic molecular structures dye are inert and difficulty biodegradable and harmful to aquatic life in rivers. The occupational exposure of workers in the textile industries is linked to a higher bladder cancer risk. The use of hair coloring products and breast cancer has also been linked [2-4].

* Corresponding author

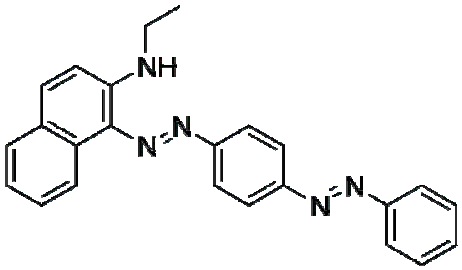

FIGURE 1 - Chemical structure of Sudan Red.

The group of color additives known as Sudan dyes (Fig.1) consists of a number of red colors, e.g., Sudan I through IV, Sudan Orange G, Sudan Red B, Sudan Red G, and Sudan Red 7B. Since their degradation products carcinogens and teratogens, their application as food-additives is forbidden. However, in some countries, these dyes are still occasionally used to intensify the color of bell pepper and chili powders. The EU-Rapid Alert System (RASFF) disseminated a series of notifications concerning the presence of Sudan dyes in chili products and other foods (spices, tomato sauces, pastas and sausages) [5]. Synthetic dyes treatment from wastewater before discharging to environment before their offering to public use is essential for the protection of health and environment is required. Some of the techniques used in treatment of wastewaters containing dyes are flocculation, coagulation, precipitation, adsorption, membrane filtration, electrochemical techniques, ozonation and fungal decolorization [6]. Among these techniques, adsorption is an effective technique in term of efficiency, capacity and large scale applicability to as well as the regeneration recovery and recycling potential of adsorbents [6–10]. Some commercial systems currently use activated carbon as an adsorbent to remove dyes in wastewater [11-14]. However, the high cost of activated carbon and high removal times restricts its comprehensive use. Although the adsorption behaviors of aromatic adsorbate on gold and silver nanoparticle surfaces have been extensively investigated, the enhancement mechanism is not completely understood. In this paper, we describe the adsorption of SR7B from aqueous solutions onto this Ag-NP-AC adsorbent has reported. Equilibrium

adsorption isotherms were measured and the experimental data were analyzed to commonly used models including Langmuir, Freundlich, Tempkin and Dubinin- Radushkevich isotherm equations.

2. MATERIALS AND METHODS

2.1. Instruments and Reagents.

Sudan red 7B (Merck, Darmstadt, Germany) stock solution was prepared by dissolving require amount of its solid material in double distilled water. The test solutions daily were prepared by diluting their stock solution to the desired concentrations. The pH measurements were done using pH/Ion meter model-682 (Metrohm, Switzerland, swiss) and absorption studies were carried out using Jusco UV-Visible spectrophotometer model V-570. All chemicals include KOH, HNO_3, KCl from Merck (Darmstadt, Germany).

2.2. Measurements of dye uptake.

Concentrations of SR7B in solution were estimated quantitatively using the linear regression equations obtained by plotting its calibration curve over a range of concentrations. The dye adsorption capacities of adsorbent were determined at the time intervals in the range of 0-35 min and at various temperatures (10–60 ◦C). The equilibrium was established after 15 min for SR7B respectively. The effect of initial pH on both dyes adsorptions was studied at initial concentration of 10 mg L^{-1} in the pH range of 2-9 by the addition of HCl or KOH. Dye adsorption experiments were also accomplished to obtain isotherms at room temperatures in SR7B concentration range of 5–100 mg L^{-1}. The amount of dye adsorbed by adsorbent, q_e (mg g^{-1}), was calculated by the following mass balance relationship:

$$q_e = (C_0 - C_e)\, V/W \quad (1)$$

Where C_0 and C_e are the initial and equilibrium dye concentrations in solution, respectively (mg L^{-1}), V the volume of the solution (L) and W is the mass (g) of the adsorbent used.

2.3. Preparation of SNPC

MWNTs were treated according to the previous procedure [13]. Nano-silver coated multi-walled carbon nanotubes were prepared by chemical plating method [14]. Firstly, 1.0 g purified and functionalized MWNTs was mixed with 50mL mixture solution of 38% formaldehyde, absolute ethyl alcohol and double distilled water (volumetric ratio 3:10:10). Secondly, 50mL mixture solution of 35 g L^{-1} silver nitrate ($AgNO_3$) solution and 25% ammonia solution (volumetric ratio1:2) was dropped one by one into the mixture of MWNTs–formaldehyde–alcohol–water solution. Keeping the pH value of reacted solution is 8–9, the reaction is processed under strong stirring. After reaction, the product is centrifugated and washed by double distilled water twice, dried in vacuum oven at 60◦C [15, 16].

3. RESULTS AND DISCUSSION

3.1. Structural properties and amount of Ag NP- AC

Figure 2A shows the UV-Vis absorption spectra correspond to surface plasmon resonance (SPR) of Ag nanoparticle obtained at different time intervals after mixing $AgNO_3$ aqueous solution with soluble formaldehyde aqueous solution at 50 °C. The maximum SPR at 400 nm was achieved after 24 h [17]. The broadband indicates a relatively high polydispersity, both in size and shape of the Ag particles.

X-ray diffraction (XRD) pattern of silver nanoparticles powder is shown in Figure 2B. The pattern exhibits peaks at 2θ angles of 38.17, 44.21, 64.32, and 77.12 that correspond to the [111], [200], [220], and [311] crystal planes of a cubic lattice structure of silver nanoparticles, respectively [18]. From the full-width at half-maximum of diffraction peaks, the average size of the silver nanoparticles has been calculated using the Debye-Scherrer equation [19]. The calculated average size of Ag nanoparticles was around 55 nm.

The FESEM image of the Ag nanoparticles(Fig. 2C) show the semi-spherical in shape and quite uniform in size distribution of Ag nanoparticle in the range of 15–80 nm that has good agreement with that determined by the XRD results.

3.2. Effect of contact time

The studies involving different contact time helps in determining the uptake capacities of the dye at varying time intervals at fixed value of adsorbents. Adsorption of SR7B onto Ag-NP-AC was monitored spectrophotometrically by the procedure described above. Absorbance data, obtained in 1-min intervals until equilibrium, were converted into concentration data using the corresponding calibration relations [10]. It was established (0.02 g), 15 min of contact time was found sufficient to acquire equilibrium. Within the first 5 min almost 99 % adsorption occurred for Ag NP-AC (Fig. 3). The adsorption rate was found to decrease with increase in time [20].

3.3. Effect of pH

The pH is one of the most important parameters in controlling the adsorption process. The pH of the solution was controlled by the addition of HCl or NaOH. The effect of pH on the adsorption of SR7B ions on Ag-NP-AC is shown in Figure 4. The uptake of SR7B ions was minimum at pH 3 and maximum at pH 4. However, when the pH of the solution was increased (more than pH 4), its uptake was increased. It appears that a change in pH of the solution results in the formation of different ionic species. It seems that SR7B can be absorbed on Ag-NP-AC via soft-soft interaction with silver atom of adsorbent

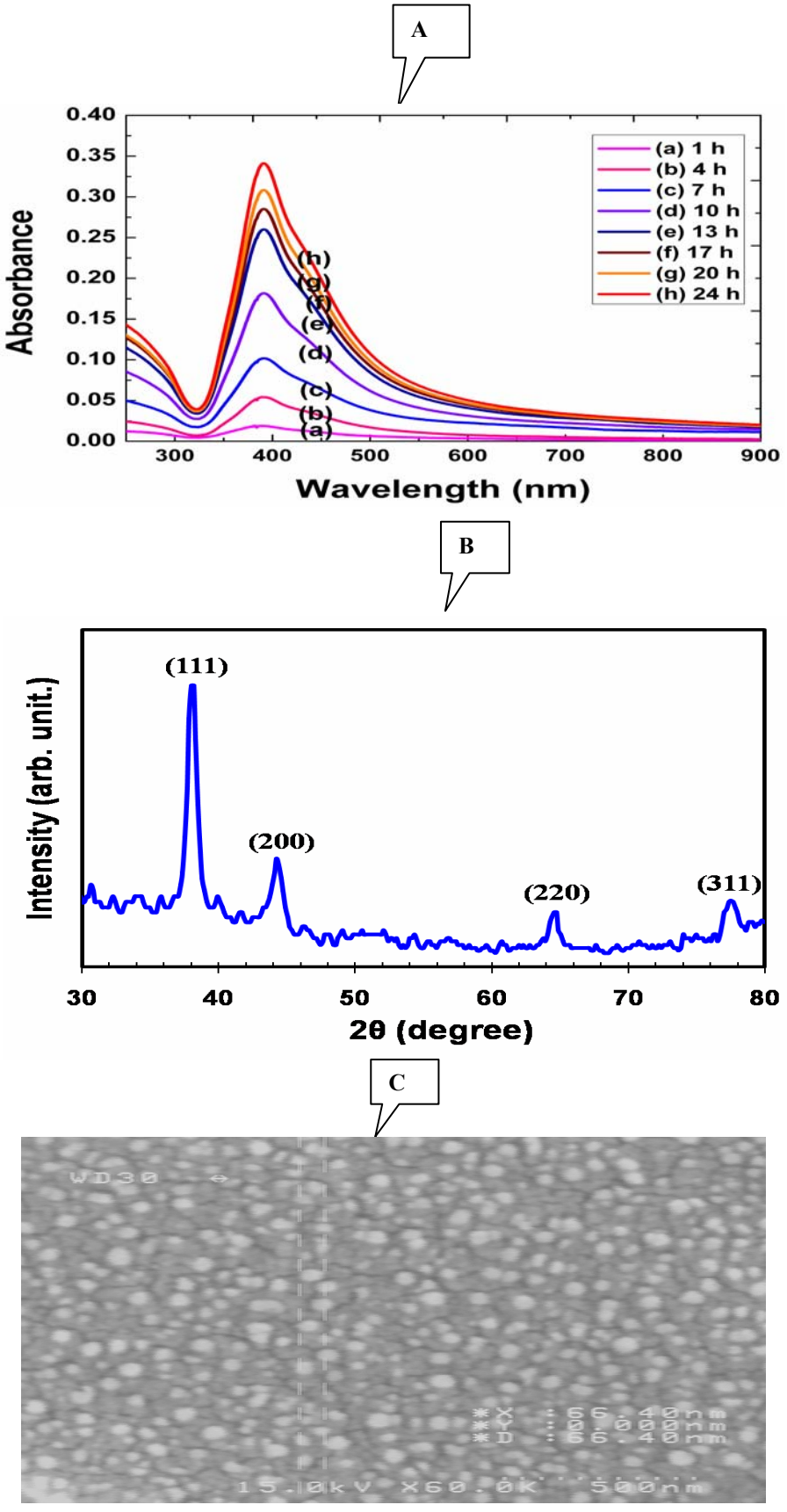

FIGURE 2 - A (Temporal evolution of UV-visible absorption spectra after addition of $AgNO_3$ solution into soluble formaldehyde solution at 50 °C), B (X-ray diffraction pattern of the starch-stabilized Ag Nanoparticles), C (FESEM image of the Ag nanoparticles loaded onto activated carbon).

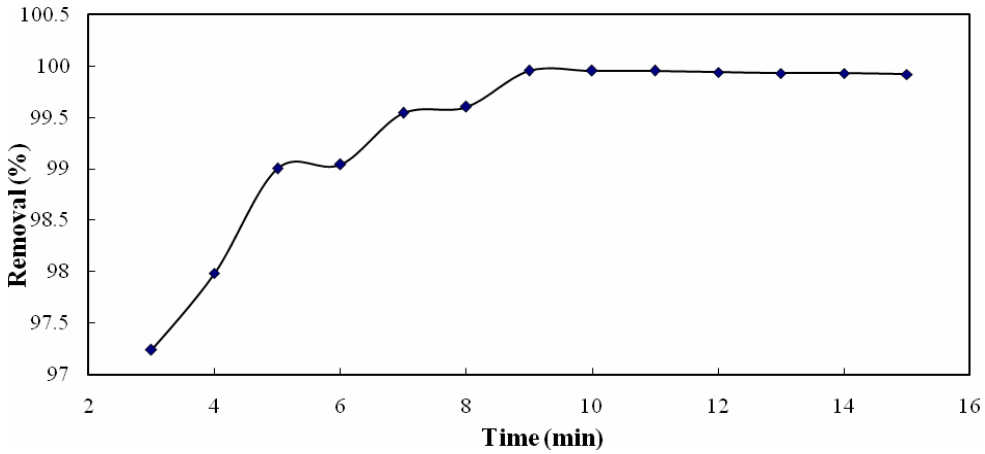

FIGURE 3 - Effect of contact time of removal of Sudan Red 7B

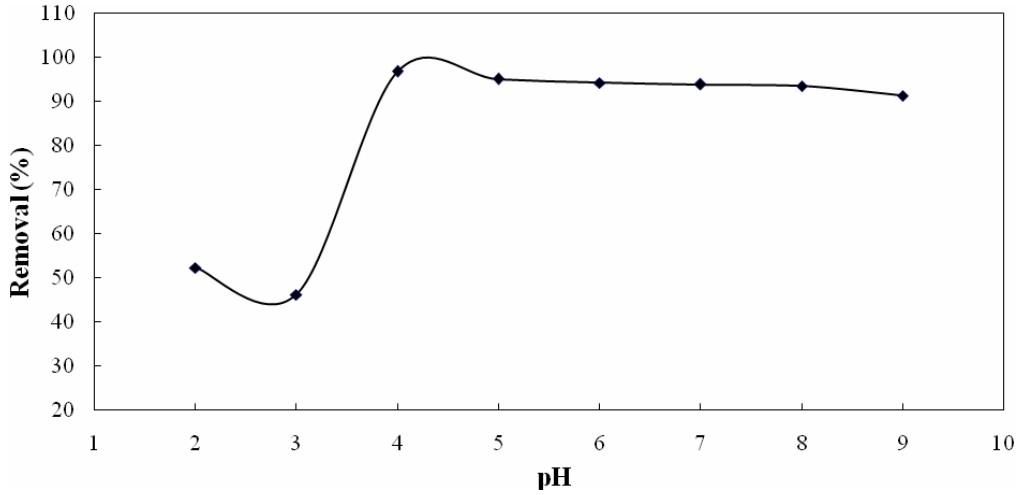

FIGURE 4 - Effect of pH on the removal of Sudan Red 7B at room temperature.

or via hydrogen bonding with various functional group of AC. At lower pH, the AC functional group and SR7B molecules get positive charge and due to repulsive force removal percentage decrease. At higher pH, functional group pf AC and SR7B deprotonated and the strong interaction of SR7B with nano silver particle with high surface area was achieved.

At pH value higher than 4, the existence of Ag-NP-AC surface OH- creates a competition between ionic dye and decreases the aggregation of SR7B [21-25].

3.4. Effect of amount of Ag-NP-AC on SR7B removal percentage

The amount of Ag-NP-AC is determines the capacity of adsorbent for a given initial concentration of dye solution. The effect of amount of Ag-NP-AC on the SR7B removal percentage is shown in Fig. 5. It was observed that initially the removal percentage increased rapidly with the increase in amount of Ag-NP-AC and after 0.02 g for 50 mL SR7B solution the removal percentage almost reached a constant value. The SR7B removal percentage increased from 90% to 99% respectively with the increase of adsorbent dose from 0.02-0.09 g. The increase in dye removal percentage was due to increased available sorption surface such as silver atom and AC functional group and the availability of more adsorption sites [26]. This may be attributed to the increase in the availability of surface active sites resulting from the increased dose and conglomeration of the adsorbent [27, 28]. When the adsorbent dose was increased to 0.02 g, the ratio of SR7B adsorbed to adsorbent showed no significant difference. Therefore, 0.4 g/L of adsorbent was chosen for later studies [29].

3.5. Effect of Initial Dye Concentration.

The effect of the initial SR7B concentration in the range of (5.0 to 100.0) mg L-1 on its adsorption rate and amount of adsorbed SR7B onto Ag NP-AC was studied in the pH of 4.0 and 0.02 gL-1 of Ag NP-AC. It was seen that, increasing the initial SR7B concentration (the con-

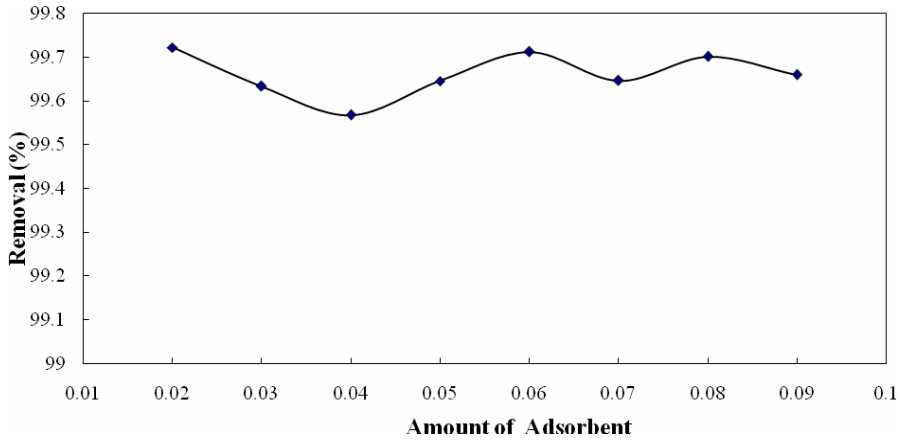

FIGURE 5 - Effect of amount of adsorbent on Sudan Red 7B removal at dye at pH and room temperature.

centration was a driving force of mass transfer) at the initial stage of adsorption lead to improvement and increase in the rate of adsorption. As shown the amount of uptaked SR7B is en-hanced with increasing initial dye concentration. By increasing the initial dye concentration, the SR7B removal percentage in despite the actual amount of adsorbed SR7B per unit mass of proposed adsorbent significantly decreased [30].

3.6. Adsorption isotherms

Adsorption from the liquid phase was carried out to verify the nature, porosity and the capacities of the samples. Sudan red (SR7B) were employed as the adsorbates in the adsorption experiments. An aqueous solution with a concentration of 500 mg/l was prepared by mixing an appropriate amount of SR7B with distilled water adsorption experiments were conducted by placing 0.02 g of the Ag-NP-AC samples and 50 ml of the aqueous solution in a 250 ml glass-stoppered flash. The flask was then put in a constant-temperature shaker bath with a shaker speed of 300 rpm. The isothermal adsorption experiments were performed at 25 ±2°C [31].

After reaching the equilibrium, the experimental data was fitted to conventional models such as Langmuir, Freundlich and Tempkin isotherms and their constants were calculated. The Langmuir isotherm is based on the assumptions that the molecules of the adsorbate are adsorbed at well-defined, energetically equal sites without interacting with each other, and each site can hold only one molecule [32].

The dimensionless separation factor showing the favorability and the shape of the adsorption isotherms by applying the following equation:

$$r = 1/(1 + bC_o) \qquad (2)$$

Where b signifies the Langmuir constant and C_o is the initial concentration. It was seen that all the r-values obtained (Table 1) are less than unity, confirming that adsorption process is favored for both absorbents.

The equation of Langmuir isotherm is represented as follows:

$$q_e = K_L q_m C_e /(1 + K_L C_e) \qquad (3)$$

where C_e is the equilibrium concentration (mg/L), q_e is the amount of adsorbents sorbed per unit mass of adsorbent at equilibrium (mg/g), q_m is the theoretical maximum adsorption capacity (mg/g), K_L is the Langmuir isotherm constant related to the energy of adsorption (L/mg). A well-known linear expression for the Langmuir isotherm is represented as follows:

$$1/q_e = 1/q_m + 1/K_L q_m C_e \qquad (4)$$

The values of K_L and q_m can be determined from the slope and intercept of the linear plot of C_e/q_e versus C_e [33].

The validity of Freundlich adsorption model was established using the following relation: $\log q_e = \log K_F + (1/n) \log C_e$ (5)

where q_e is the amount adsorbed (g), C_e the equilibrium concentration of the adsorbate, and K_F and n are the Freundlich constants related to the adsorption capacity and adsorption intensity, respectively clearly revealed that $\log C_e$ versus $\log q_e$ plots gave straight lines. Freundlich constants derived from these straight lines are presented in Table 1.

Tempkin isotherm takes into account the effects of indirect adsorbate–adsorbate interactions on adsorption, and suggests that the heat of adsorption of all the molecules in the layer would decrease linearly with coverage due to these interactions [34]. The linear form of Tempkin isotherm is expressed as follows:

$$q_e = B \ln A + B \ln C_e \qquad (6)$$

Where B is the Tempkin constant related to heat of adsorption and A is he equilibrium binding constant (L mg^{-1}). The constants A and B can be determined by a plot of q_e versus ln C_e (Table 1) [32].

TABLE 1 - Isotherm constant parameters and correlation coefficients calculated for the adsorption

Isotherm	Equation	Plot	parameters	SR7B
Langmuir-1:	$1/q_e = 1/(K_aQ_mC_e) + 1/Q_m$	A plot C_e/q_e versus C_e should indicate a straight line of slope $1/Q_m$ and an intercept of $1/(K_aQ_m)$.	Q_m(mg/g)	90.91
			K_a (L mg^{-1})	0.52
			R^2	0.985
Freundlich:	$\ln q_e = \ln K_F + (1/n) \ln C_e$	The values of K_f and 1/n were determined from the intercept and slope of linear plot of ln qe versus ln Ce, respectively.	1/n	0.23
			K_F (L/mg)	39.26
			R^2	0.905
Tempkin:	$q_e = B_1 \ln K_T + B_1 \ln C_e$	Values of B_1 and K_T were calculated from the plot of qe against ln C_e.	B_1	13.13
			K_T (L/mg)	18.52
			R^2	0.889
Dubinin and Radushkevich (D-R):	$\ln q_e = \ln Q_s - B\varepsilon^2$	The slope of the plot of ln q_e versus ε^2 gives K (mol^2 $(kJ^2)^{-1}$) and the intercept yields the adsorption capacity, Q_m (mg g^{-1}).	Q_s (mg/g)	59.3
			B	2E-07
			E (kj/mol) = $1/(2B)^{1/2}$	1581.1
			R^2	0.77

TABLE 2 - Kinetic parameters for the adsorption of SR7B onto adsorbent.

Model	Equation	Plot	Parameters	SR7B
First-order kinetic	$\text{Log}(q_e - q_t) = \log(q_e) - (k_1/2.303)t$	Plot the values of log ($q_e - q_t$) versus t to give a linear relationship from which k_1 and q_e can be determined from the slope and intercept, respectively.	k_1	0.44
			q_e (calc)	2.53
			R^2	0.962
Second-order kinetic	$(t/q_t) = 1/(k_2q_e^2) + 1/q_e (t)$	Plot the values of (t/q_t) versus t to give a linear relationship from which k_1 and q_e can be determined from the slope and intercept, respectively.	k_2	0.51
			q_e (calc)	25.6
			R^2	0.99
			h	37.0
Intraparticle diffusion	$q_t = K_{dif}\, t^{1/2} + C$	The values of K_{dif} and C were calculated from the slopes of qt versus $t^{1/2}$.	K_{diff}	0.52
			C	23.48
			R^2	0.935
Elovich	$q_t = 1/\beta \ln(\alpha\beta) + 1/\beta \ln(t)$	Plot the values of (q_t) versus ln(t) to give a linear relationship from which α and β can be determined from the slope and intercept, respectively.	β	2.5
			R^2	0.85
q_e (exp)				24.98

3.7 Kinetic studies

The behavior of the SR7B adsorption is analyzed using the Lagergren first-order kinetic model, pseudo second-order kinetic model and intraparticle diffusion [35].

A linear form of the Lagergren first-order model expression is:

$$\log (q_e\text{-}q_t) = \log q_e\text{-}(k_1 t/ 2.303)t \quad (7)$$

Where q_e and q_t (mg·g^{-1}) are the amount adsorbed at equilibrium and time t (min), respectively, k_1 (min^{-1}) is the rate constant of Langergren first-order adsorption (min^{-1}). The values of log (q_e-q_t) were calculated from the kinetic data.

The kinetic data are further analyzed using the pseudo second-order kinetics expressed as:

$$t/q_t = (1/k_2q_e^2) + (1/q_e)t \quad (8)$$

Where k_2 (g·mg^{-1}·min^{-1}) is the rate constant of pseudo second-order adsorption. If the second-order kinetics is applicable, the plot of t/q_t versus t should give a linear relationship and it is not needed to know any parameter beforehand.

The adsorbate species are most probably transported from the bulk of the solution into the solid phase with an intraparticle diffusion process, which is often the rate-limiting step in many adsorption processes. The possibility of intraparticle diffusion is explored by using the intraparticle diffusion model [36],

$$q_t = k_{id}t^{1/2} + C \quad (9)$$

Where C is the intercept and k_{id} is the intraparticle diffusion rate constant from the plot of q_t versus $t^{1/2}$, the values kid, C and the corresponding linear regression correlation coefficient R^2 are given in Table 2 that show the intraparticle rate constants calculated are 0.516 mg·g^{-1}·$min^{-1/2}$ [37].

4. CONCLUSIONS

Based on the experimental results, the following conclusions can be made:

1. Ag-NP-AC shows excellent adsorption potential for SR7B removal.

2. The Langmuir and Freundlich isotherm parameters confirmed that the adsorption of SR7B onto Ag-NP-AC was favorable and improved by increase in pH, concentration, temperature, speed of agitation and amount of Ag-NP-AC.

3. The Langmuir isotherm model and Ho's pseudo-second order model were found to be the best fitting isotherm and kinetic models.

4. The proposed sorbent with high adsorption capacity and short analysis time is a suitable for waste water treatment.

REFERENCES

[1] Park, H. and Choi, W. (2003) Visible light and Fe(III)-mediated degradation of acid Orange 7 in the absence of H_2O_2, J. Photochem. Photobiol. A. Chem. 159 241– 247.

[2] Ghaedi M., Hassanzadeh, A. and Nasiri Kokhdan, S. (2011) Multiwalled Carbon Nanotubes as Adsorbents for the Kinetic and Equilibrium Study of the Removal of Alizarin Red S and Morin, J. Chem. Eng. Data. 56, 2511-2520.

[3] Zheng, T., Holford, TR., Mayne, ST., Owens, PH., Boyle, P., Zhang, B. (2002) Use of hair colouring products and breast cancer risk: a case-control study in Connecticut. Eur. J. Cancer. 38, 1647–1652.

[4] Ho, Y-S., Chiang, T-H. and Hsueh, Y-M. (2005) Removal of basic dye from aqueous solution using tree fern as a biosorbent Process. Biochem. 40,119–124.

[5] Souka, N. Farag, A. N. (1990) Dosimetric studies based on the radiation-induced bleaching of Sudan red and Sudan blue dyes in organic solutions. International Journal of Radiation Applications and Instrumentation. Part A. Applied Radiation and Isotopes, 41(8)739-744.

[6] Dabrowski, A. (2001) Adsorption from theory to practice, Adv. Colloid Interface 93, 135–224.

[7] Choy, K.K.H., Porter, J.F. and McKay, G. (2004) Intraparticle diffusion in single and multicomponent acid dye adsorption from wastewater onto carbon, Chem. Eng. J. 103, 133–145.

[8] Robinson, T., McMullan, G., Marchant, R. and Nigam, P. (2001) Remediation of dyes in textile effluents; a critical review on current treatment technologies with a proposed alternative, Bioresource Technol. 77, 247– 255.

[9] Chern, J.M. and Wu, J.Y. (2001) Desorption of dye from activated carbon beds: effects of temperature, pH, and alcohol, Water Res. 35, 355–368.

[10] Hoda, N., Bayram, E. and Ayranci, E. (2006) Kinetic and equilibrium studies on the removal of acid dyes from aqueous solutions by adsorption onto activated carbon cloth, J. Hazard. Mater.B137, 344–351.

[11] Santhy, K. and Selvapathy, P. (2006) Removal of reactive dyes from wastewater by adsorption on coir pith activated carbon, Bioresour. Technol. 97 1329–1336.

[12] Walker, G.M. and Weatherley, L.R. (1997) Fixed bed adsorption of acid dyes onto activated carbon,Water Res. 31 (8) 2093–2101.

[13] Li, Y., Gao, B., Wu, T., Wang, B. and Li, X. (2009) Adsorption properties of aluminum magnesium mixed hydroxide for the model anionic dye Reactive Brilliant Red K-2BP, J. Hazard. Mater.164, 1098–1104.

[14] Hosseini, S. J., Nasiri Kokhdan, S., Ghaedi, A. M., Moosavian, S. S., (2011) Comparison of Multiwalled Carbon Nanotubes and Activated Carbon for efficient removal of methyl orange: kinetic and thermodynamic investigation. Fresen. Environ. Bull., 20, 219-234.

[15] Hiura, H., Ebbesen, T. W., Tanigaki, K. (1995) Opening and purification of carbon nanotubes in high yields. Adv. Mater. 7, 275-276.

[16] Wu, H. P., Wu, X. J., Ge, M. Y., Zhang, G. Q., Wang, Y.W., Jiang, J. (2007) Properties investigation on isotropical conductive adhesives filled with silver coated carbon nanotubes. Compos. Sci. Technol. 67, 1182–1186.

[17] Huang, H. and Yang, X. (2004) Synthesis of polysaccharide-stabilized gold and silver nanoparticles: a green method, Carbohyd. Res. 339, 2627-31.

[18] Wang, X. Chen, Y. (2008) A new two-phase system for the preparation of nearly monodisperse silver nanoparticles, Mater. Lett. 62, 4366–8.

[19] Goudarzi, A. Motedayen Aval, G. Park, S. S. Choi, M.C. Sahraei, R. Habib Ullah, M. Avane, A. and Ha, C. S. (2009) Low-Temperature Growth of Nanocrystalline Mn-Doped ZnS Thin Films Prepared by Chemical Bath Deposition and Optical Properties, Chem. Mater. 21, 2375-2385.

[20] Mittal, A., Malviya, A., Kaur, D., Mittal, J. and Kurup, L. (2007) Studies on the adsorption kinetics and isotherms for the removal and recovery of Methyl Orange from wastewaters using waste materials, Journal of Hazardous Materials 148, 229–240.

[21] Ghaedi, M. Tashkhourian, J. Amiri Pebdani, A. Sadeghian, B. Nami Ana, F. (2011) Equilibrium, kinetic and thermodynamic study of removal of reactive orange 12 on platinum nanoparticle loaded on activated carbon as novel adsorbent, Korean J. Chem. Eng. 28 2255-2261.

[22] Ghaedi, M. Zamani Amirabad, S. Marahel, F. Nasiri Kokhdan, S. Sahraei, R. Daneshfar, A. (2011) Synthesis and characterization of Cadmium selenide nanoparticles loaded on activated carbon and its efficient application for removal of Muroxide from aqueous solution, Spectrochim. Acta Part A: Mol. Biomol. Spectrosc. 83,46–51.

[23] Arivoli, S., Kalpana, K., Sudha, R. and Rajachandrasekar, T. (2007) Comparative Study on the Adsorption Kinetics and Thermodynamics of Metal Ions onto Acid Activated Low Cost Carbon", E. J. Chem., 4, 238–254.

[24] Guo, Y., Zhao, J., Zhang, H., Yang, S., Wang, Z. and Xu, H. (2005) Use of Rice Husk Based Porous Carbon for the Adsorption Rhodamine B from Aqueous Solution, Dyes and Pigments, 66 123–128.

[25] Ghaedi, M. Tavallali, H. Sharifi, M. Nasiri Kokhdan, S. Asghari, A. Preparation of low cost activated carbon from Myrtus communis and pomegranate and their efficient application for removal of Congo red from aqueous solution, Spectrochim. Acta Part A: Mol. Biomol. Spectrosc. 86 (2012) 107–114.

[26] Ghaedi, M., Shokrollahi, A., Hossainian, H., Nasiri Kokhdan, S., (2011) Comparison of Activated Carbon and Multiwalled Carbon Nanotube for efficient removal of Eriochrome Cyanine R: Kinetic, Isotherm and Thermodynamic study of removal process, J. Chem. Eng. Data, 56, 3227-3235

[27] Kannan, N. Sundaram, M.M. (2001) Kinetics and mechanism of removal of methylene blue by adsorption on various carbons—a comparative study, Dyes Pigments 51(1) 25–40.

[28] Garg, V.K., Gupta, R., Yadav, A.B., Kumar, R. (2003) Dye removal from aqueous solution by adsorption on treated sawdust, Bioresour. Technol. 89 121–124.

[29] Chen, S., Zhang, J., Zhang, C., Yue, Q., Li, Y. and Li, C. (2010) Equilibrium and kinetic studies of methyl orange and methyl violet adsorption on activated carbon derived from Phragmites australis, Desalination 252, 149–156

[30] Colak, F., Atar, N. and Olgun, A. (2009) Biosorption of acidic dyes from aqueous solution by Paenibacillus macerans: Kinetic, thermodynamic and equilibrium studies, Chem.Eng. J. 150, 122–130.

[31] Bouchemal, N. and Addoun, F. (2009) Adsorption of dyes from aqueous solution onto activated carbons prepared from date pits: The effect of adsorbents pore size distribution, Desalination and Water Treatment 7 242–250.

[32] Won, S.W., Wu, G., Ma, H., Liu, Q., Yan, Y., Cui, L. and Yu, Y.S. (2006) Performance and mechanism in adsorption of Reactive Red 4 by solid waste from coke wastewater treatment plant. Waste Manag. 24 (4), 299–300.

[33] El-Geundi, M.S. (1991) Color removal from textile effluents by adsorption techniques. Water Res. 25 (3), 271–273.

[34] Hameed, B.H. (2009) Spent tea leaves: A new non-conventional and low-cost adsorbent for removal of basic dye from aqueous solutions. J. Hazard. Mater. 161 (2-3), 753-759.

[35] Namasivayam, C., Yamuna, R.T., (1995) Adsorption of direct red 12 B by biogas residual slurry: Equilibrium and rate processes, Environ. Pollut., 89 (1), 1-7.

[36] Bulut, Y. and Aydin, H. (2006) A kinetics and thermodynamics study of methylene blue adsorption on wheat shells, Desalination, 194 (1-3), 259-267.

[37] Ghaedi, M. Khajesharifi, H. Yadkuri, A. H. Roosta , M. Sahraei , R. Daneshfar, A. (2012) Cadmium hydroxide nanowire loaded on activated carbon as efficient adsorbent for removal of Bromocresol Green, Spectrochim. Acta Part A: Mol. Biomol. Spectrosc. 86 62– 68.

Received: July 04, 2011
Revised: August 09, 2011
Accepted: September 09, 2011

CORRESPONDING AUTHOR

Farzaneh Marahel
Chemistry Department,
Islamic Azad University
Omidiyeh Branch, Omidiyeh
IRAN

Phone: (0098)-741 2223048
Fax: (0098)-741 2223048
E-mail: farzanehmarahel@yahoo.com